Analytica Chimica Acta xxx (xxxx) xxx

Contents lists available at ScienceDirect

Analytica Chimica Acta

journal homepage: www.elsevier.com/locate/aca

A new aptamer/black phosphorous interdigital electrode for malachite green detection

Lidong Wu [a, *], Zhiyuan Xu [c], Qingyi Meng [c], Yushi Xiao [a, b], Qiang Cao [a, b], Brijesh Rathi [d], Huan Liu [a], Gang Han [a], Jing Zhang [c], Jiang Yan [c]

[a] Key Laboratory of Control of Quality and Safety for Aquatic Products, Chinese Academy of Fishery Sciences, Beijing, 100141, China
[b] College of Food Science and Technology, Shanghai Ocean University, Shanghai, 201306, China
[c] College of Information, North China University of Technology, Beijing, 100043, China
[d] Department of Chemistry, Hansraj College University of Delhi, Delhi, 110007, India

HIGHLIGHTS

- The interdigital electrode is suitable for large scale production of sensors.
- This sensor can make malachite green (MG) detection on-site, portable and reliable.
- The cysteine coating BP is a prefect material for cationic dye detection.
- The sensor has a lowest detection limit of 0.3 ng L^{-1} toward MG.

GRAPHICAL ABSTRACT

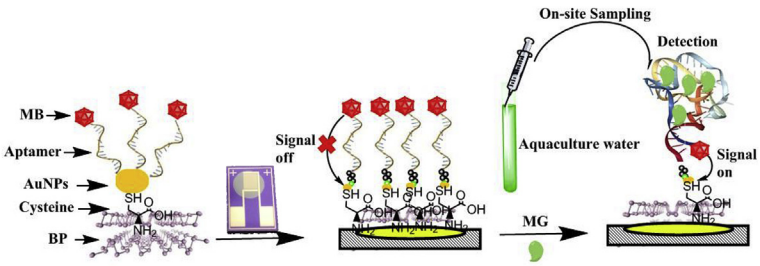

ARTICLE INFO

Article history:
Received 26 October 2019
Received in revised form
5 November 2019
Accepted 9 November 2019
Available online xxx

Keywords:
The CYS-BP-AuNP nanocomposite
Aptamer
Malachite green
Portability
Interdigital electrode

ABSTRACT

Malachite Green (MG), a cationic triphenylmethane dye, has adverse effects on the immune and reproductive system. Thus, it is essential to develop a rapid, sensitive and high-selective method for determination of MG. Black phosphorus (BP) has high charge-carrier mobility (~1000 cm^2 V^{-1} s^{-1}) and high adsorption capacity for cationic dyes (i.e. MG) through both electrostatic and hydrophobic interactions. Thus, it potentially plays as a high-sensitive sensing platform for detecting MG. However, BP degrades within 12 h under humid condition, which limits its applications. To overcome this issue, cysteine (CYS) is used for protecting BP from oxidation and ceasing its degradation. To the best of our knowledge, it is the first time that CYS is used to functionalize BP, and a silicon interdigital electrode is fabricated with the functionalized BP and aptamer. The BP-based interdigital electrode shows a lowest detection limit of 0.3 ng L^{-1} toward MG. This work provides a new route to prepare a large scale and selective biosensor for MG monitoring on site in future.

1. Introduction

Malachite Green (MG), a cationic triphenylmethane dye, is widely disseminated within the aquaculture water and forbidden in food [1,2]. Especially, it is widely polluted in aquaculture water in Asia and Africa. Due to its adverse effects on water ecology and human health [3], there are increasing concerns about MG polluted water [4]. Thus, it is essential to develop a rapid, sensitive and high-selective method for determination of MG.

Electrochemical biosensors are ideally analytical tools for on-

* Corresponding author.
E-mail address: lidongwu@mit.edu (L. Wu).

https://doi.org/10.1016/j.aca.2019.11.026
0003-2670/

site monitoring MG due to its cost-effectiveness, portability and reliability. Biosensing materials play a vital role in the development of electrochemical biosensors [5,6]. Designing the superior biosensing material is the core technology of electrochemical biosensors for improving limit of detection (LOD) and sensitivity. Black phosphorus (BP) has been recognized as a rising star of two-dimensional (2D) material and a potential biosensing material [7–9]. Due to its thickness-dependent bandgap ranging from 0.3 to 2.0 eV [10], and high charge carrier mobility (approximately 1000 $cm^2 V^{-1} s^{-1}$) [11], it has been applied in gas sensors [12,13], and field effect transistors [14–16]. Zhang's Group has reported that BP had high adsorption capacities for cationic dyes (i.e. MG or methylene blue (MB)) through electrostatic and hydrophobic interactions [17]. Thus, the strong sorption ability of BP with MG (target molecule) and MB (common electrochemical signal molecule) could enrich the target and signal molecule on the electrode and improve the sensitivity of the electrochemical biosensor.

Despite BP is recognized as one of the most thermodynamically stable allotrope of phosphorus, it is still severe degradation under ambient oxygen and water [18,19]. The raw BP can fast transform into PO_3^{3-} or PO_4^{3-} within 12 h, and the degradation of BP is most likely to occur at the edges of BP [16]. In the first step, the edge sites of BP react with oxygen ($P \rightarrow P_xO_y$). In the second step, water enables P_xO_y to transform into the final anions (PO_4^{3-}) [20,21]. This limits the exploration of BP in electrochemical sensing.

Researchers have explored different methods to overcome the degeneration of BP under humid environment, including encapsulation [22], non-covalent functionalization [23,24], and covalent chemical modification [25], etc. The non-covalent functionalization of BP not only keeps its originally puckered honeycomb structure and good conductivity, but also improves BP's stability and dispersion in aqueous solution. The functionalized BP offers a promising possibility as biosensing platform in aqueous solution. Herein, L-cysteine (CYS), an antioxidant amino acid, which possesses NH_2 and SH groups, is used for non-covalent coating on the surface of BP through the electrostatic interaction between NH_2 of CYS and lone-pair electrons of BP to protect BP from oxidation and degradation.

The functionalized BP is utilized as biosensing material to improve the sensitivity and LOD of the biosensor. Meanwhile, aptamer can be a specific recognition sector to fulfill selective detection of MG. Aptamer is a single-stranded DNA or RNA with a high affinity for target and referred to as "chemical antibodies" [26,27]. In this work, the MG aptamer as a recognition sector, and the functionalized BP as a signal amplifier, and interdigital electrode as a portable detector, they work together to construct a portable, sensitive and selective interdigital electrode for MG detection. The preparation process of silicon based interdigital electrode is repeatable and well-controllable, which makes the large scale production of portable biosensor is envisioned in future.

2. Experimental section

2.1. Materials and solutions

MG, MB, CYS, DMSO, and other chemicals are purchased from Sigma Aldrich (USA). MG dissolves in H_2O to get series of standard solution. The aptamer sequences (screened by SELEX method) 5′-SH-$(CH_2)_6$-GGAUCCCGACUGGCGAGAGCCAGGUAACGAAUGGAUCC-MB-3′ is obtained from Takara Biotechnology Co. Ltd. (Dalian, China) and dissolves in 20 mmol L^{-1} pH 8.0 PBS solution.

2.2. Apparatus

Transmission electron microscopy (TEM) and scan electron microscopy (SEM) images are obtained by a JEM-2100 (Japan) and Zeiss Sigma 300 (Germany), respectively. Atomic force microscopy (AFM) is performed using tapping mode and silicon nitride cantilever tip (Bruker, USA). Fourier transform infrared spectroscopy (FTIR) are obtained through Nicolet 6700 (Thermo, USA). Zetasizer Nano ZS (Marvern Instruments) is used to measure the zeta potential of the BP solution. The absorbance of MG and MB is quantified by a UV spectrophotometer (Jena, Specord 200 plus) at characteristic absorptions of 621 and 664, respectively. Cyclic voltammetry (CV) and differential pulse voltammetry (DPV) is operated by a CHI 660B electrochemical workstation (CHI Instruments Inc.).

2.3. Preparation of BP, the CYS coating BP (CYS-BP) and the BP-AuNP nanocomposite

The preparation process of BP can be divided into several steps, and are operated in the acrylic glove box. There is a 1% oxygen and water in glove box, which is necessary for uniform oxidation and hydroxylation of BP. Firstly, the bulky black phosphorus is ultrasonication-assisted exfoliation in DMSO under nitrogen gas to remove the dissolved oxygen molecules. After 8000 rpm centrifugation for 20 min, BP collects from supernatant. Secondly, BP (1 mg mL^{-1}) transfers into DMSO with 1% CYS in a glass vial. Subsequently, it is capped and placed inside the silicone oil at 130 °C for 20 min. Finally, A uniform CYS protection monolayer is formed on the BP surface (CYS-BP).

Preparation of gold nanoparticles and the BP nanocomposite (BP-AuNP): 50 mL 0.1 mg L^{-1} chloroauric acid and 2.5 mL vitamin C (4 mg mL^{-1}) are mixed together for 2 h, and then 0.5 mL sodium citrate (10 mg mL^{-1}) is added into the solution to stop the reaction. The gold nanoparticles are obtained. 0.25 mg mL^{-1} functionalized BP solution (50 mL) is mixed with 0.5 mg mL^{-1} gold nanoparticles solution (50 mL), and rapidly stirred for 10 min. Through centrifugation (8000 rpm, 5 min) three times, the nanocomposite is obtained in the bottom of centrifugation vials.

MG and MB sorption experiments are performed using a vortex technique: Firstly, 2 mL of 1 mg L^{-1} functionalized BP solution is mixed with 8 mL of 2 mg L^{-1} MG or MB solution to assess the sorption ability of the functionalized BP. Secondly, the few-layered BP is separated by centrifugation at 13,000 rpm for 30 min. Finally, 2 mL of the supernatant is removed and analyzed by UV–Vis spectra.

2.4. Preparation of the BP-AuNP-Ap interdigital electrode

All the fabrication process of interdigital electrodes is completed in a super clean room to ensure the performances and yield rates of the interdigital electrodes. In order to ensure the insulation of the substrate, the silicon wafer with 300 nm SiO_2 layer is grown by thermal oxygen. The whole process is shown in Scheme 1: the BP-AuNP solution (0.5 mg mL^{-1}) is added on the interdigital electrode. Then, 8 μL, 1 μmol L^{-1} of the thiolated aptamer solution is added on the interdigital electrode for 2 h at room temperature. The weakly adsorbed aptamer is rinsed by deionized water. All the other electrodes have a similar preparation protocol with the BP-AuNP-Ap interdigital electrode.

2.5. Detection of MG by the BP-AuNP-Ap interdigital electrode

8 μL MG solution is added into PBS solution for 3 min to provide enough time for aptamer recognition of MG. And then, the BP-AuNP-Ap interdigital electrode is used for monitoring the response signal changes of MG via the DPV method.

Please cite this article as: L. Wu et al., A new aptamer/black phosphorous interdigital electrode for malachite green detection, Analytica Chimica Acta, https://doi.org/10.1016/j.aca.2019.11.026

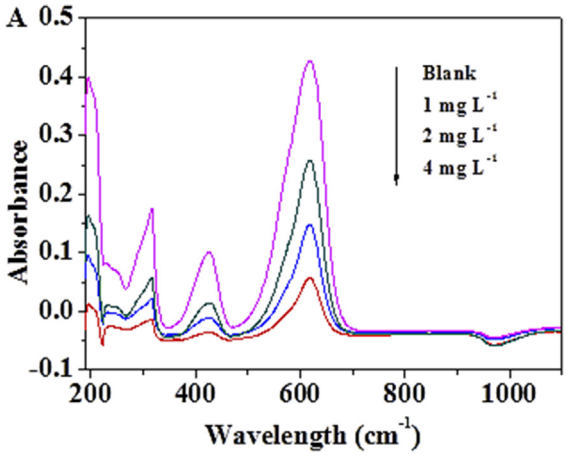

Scheme 1. Schematic diagram of the fabrication process and detection mechanism of the BP-AuNP-Ap interdigital electrode. BP is immersed in the DMSO with L-cysteine, and then the gold nanoparticles are immobilized on the BP surface through Au-S self-assembly. The BP-AuNP nanocomposite is transferred from solution to the interdigital electrode surface, and then the thiolated aptamer solution is added on the BP-AuNP nanocomposite modified interdigital electrode. The BP-AuNP-Ap interdigital electrode detects the MG molecules.

2.6. Safety considerations

MG which is classified a class II Health Hazard, can cause carcinogenic symptoms. MSDS information for these chemicals must be consulted, and precautions need to be taken for handling them (i.e., wearing gloves, eyeglasses and mask).

3. Results and discussion

3.1. BP, CYS-BP and the BP-AuNP nanocomposite characterization

The long-term stability of BP is characterized by AFM. As shown in Fig. 1A and B, the CYS-BP is stably existed in aqueous solution approximate 2 weeks. But without coating CYS, BP is degraded in aqueous solution within 12 h (Fig. 1C and D). The mechanism of BP degradation is that the edge sites of BP reacts with oxygen ($P \rightarrow P_xO_y$) and then H_2O enables P_xO_y to transform into the final anions (PO_4^{3-}) [19]. CYS as an antioxidant amino acid is used for ceasing the degradation of BP. The thickness of the functionalized BP and BP are characterized by AFM. Fig. 1E shows that the CYS thickness is approximate 0.6 nm. It indicates that there is a uniform protective layer on the BP surface. The FTIR spectra is used to verify that CYS has immobilized on the BP surface. The peak of 2550 cm^{-1} is the SH group of CYS molecules. As CYS binds on the surface of BP, the absorption bands at 1390 (symmetric stretching of −COOH), 1600 (asymmetric stretching of −COOH), and 3000-3500 cm^{-1} (NH_3^+ stretch) become weak. The change in their dipole moment is due to CYS binding with BP. These results indicate the successful modification of CYS on BP.

The structure and morphology of the functionalized BP images are obtained from TEM and SEM instruments. Fig. 2 shows the representative TEM images of the functionalized BP (A), gold nanoparticles (Figure S1) and the BP-AuNP nanocomposite (B). The raw BP degenerates in 1 min under strong electronic beam from TEM and SEM, thus the raw BP can't catch by TEM and SEM. Fig. 2A shows that the high-quality functionalized BP is obtained through the liquid-exfoliated method. Figure S1 shows the TEM image of gold nanoparticles (approximate 10 nm). Fig. 2B is the BP-AuNP nanocomposite. It is clearly shown that gold nanoparticles are dispersed on the surface of BP via Au-S self-assembly. The gold nanoparticles have covered approximate 20% of the surface of BP, and its size is around 10 nm. The structures of the functionalized BP and the BP-AuNP nanocomposite are confirmed by SEM. As shown in Fig. 2C, the high-quality functionalized BP has been prepared. Fig. 2D shows that the gold nanoparticles have dotted on the surface of BP. SEM and TEM images illustrate that the BP-AuNP nanocomposites have been prepared.

There is no absorption peak found by UV−vis spectroscopy for the supernatant. It suggests that all the functionalized BP is removed through centrifugation. As soon as the MG and MG solution adds into the functionalized BP solution, most of the MG and MB has been removed in 5 min (Figure S2). The removal efficiencies of the sorbed MG and MB is calculated through the difference

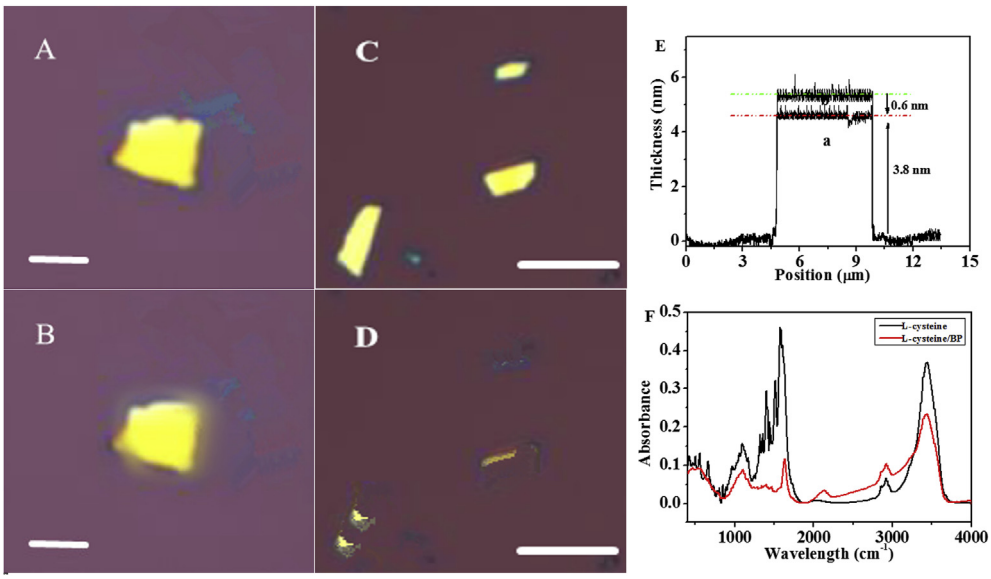

Fig. 1. Atomic force microscopy (AFM) images of (A) the functionalized BP with L-cysteine, and (B) the functionalized BP with L-cysteine in water for 12 h (Scale bar: 500 nm); and (C) BP, (D) BP in water for 12 h (Scale bar: 1.5 μm). (E) The AFM characterization of the thickness of the same BP before and after coating L-cysteine as a protective layer, the locations and the height profiles marked by dotted lines. (F) FTIR spectrum of L-cysteine and the CYS-BP.

Please cite this article as: L. Wu et al., A new aptamer/black phosphorous interdigital electrode for malachite green detection, Analytica Chimica Acta, https://doi.org/10.1016/j.aca.2019.11.026

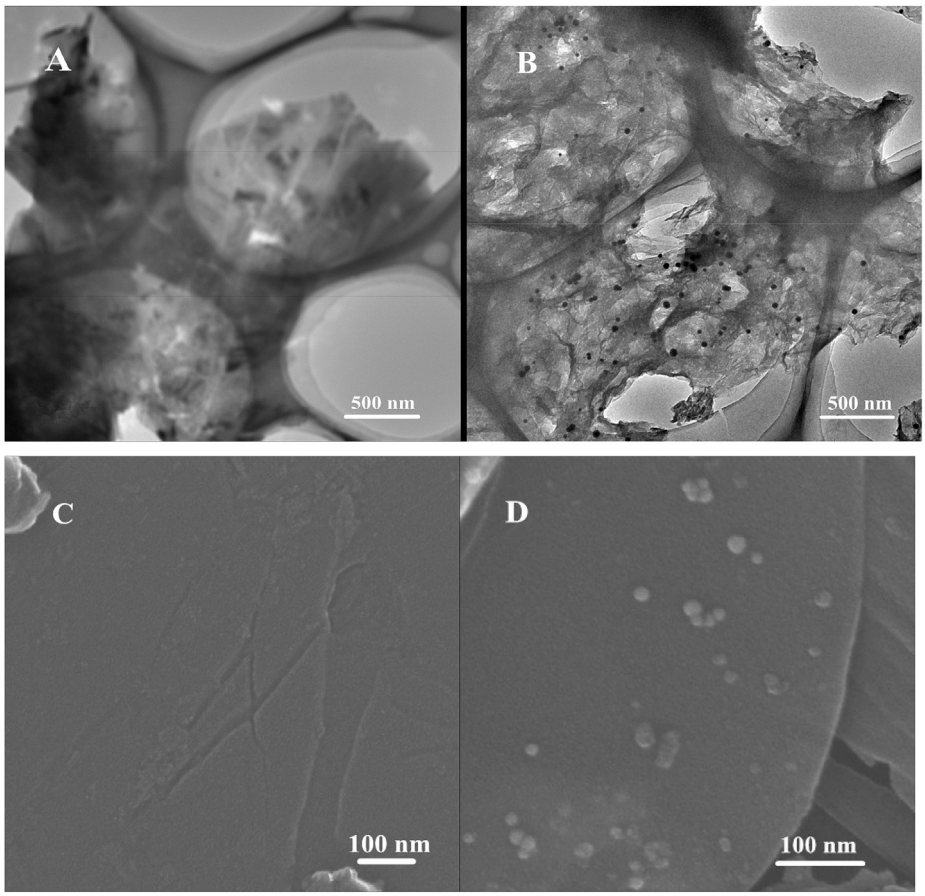

Fig. 2. TEM images of (A) BP, (B) the BP-AuNP nanocomposite. SEM images of (C) BP and (D) the BP-AuNP nanocomposite.

between initial and final concentration in aqueous solution. The absorbance peaks of both dyes (MG and MB) significantly decrease with the increase of the BP concentration. As the functionalized BP concentration increases to 4 mg L^{-1}, the sorbed percentage of MG and MB has achieved almost 90%. It indicates that BP can enrich the cationic dyes.

3.2. The immobilization process of the BP-AuNP-Ap interdigital electrode

BP has excellent charge carrier mobility (1000 $cm^2/V{\cdot}s$) and high sorption for MG [28], which plays a key role in improving the sensitivity of the interdigital electrode. In this study, CV is used for monitoring the fabrication process of the interdigital electrode. Figure S3 shows the CV signals of the bare interdigital electrode, the Ap modified interdigital electrode and the BP-AuNP-Ap interdigital electrode (curve a, curve b and curve c) in 5 mmol L^{-1} $[Fe(CN)_6]^{3-/4-}$ solution. Compare to the bare interdigital electrode, the response signal of the Ap modified interdigital electrode (curve b) decreases significantly. This is due to the thiol-aptamer covering the Au electrode surface through Au-S self-assembly. When the BP-AuNP nanocomposite and aptamers immobilize onto the interdigital electrode, the response signal increases remarkably. It is mainly due to the high conductivity of the BP-AuNP nanocomposite improving the electron transfer rate. This also indicates that the BP-AuNP nanocomposite is successfully immobilized on the interdigital electrode.

3.3. MG determined by the BP-AuNP-Ap interdigital electrode

MG is a cationic triphenylmethane dye which has been used in commercial aquaculture against the *Saprolegnia* fungus since 1936 [29]. Recently, MG has attracted the public attention due to its adverse effects on the immune and reproductive system [30,31]. Based on this reason, the BP-AuNP-Ap interdigital electrode is used for detection of MG in this research. DPV, one of the most sensitive electrochemical method, is used for monitoring the concentration of MG by the BP-AuNP-Ap interdigital electrode. The redox-active MB molecule is used for electrochemical magnification of the response signal, and its redox potential is as low as −0.25-0 V which can minimize the potential co-existed interferences [32]. Furthermore, the cationic MB and MG is easily concentrated on the negative surface charge (-29.6 ± 5.03 mV) of the functionalized BP through the electrostatic interaction [33]. Thus, BP may be an excellent platform to improve the response signal of MB and enrich the concentration of MG.

As shown in Fig. 3A, the response signal of this interdigital electrode is successively increased with adding of MG. The peak currents of the BP-AuNP-Ap interdigital electrode exhibit a linear relationship with the MG concentration from 1 ng L^{-1} to 10 μg L^{-1} (Fig. 3B), and the linear regression equation is $I = 0.0854C + 2.085$ ($R^2 = 0.995$). The LOD is calculated using the following equation: $LOD = 3\ S/m$, where S is the standard deviation, and m is the slope of calibration plot. The LOD of this interdigital electrode for MG is as low as 0.3 ng L^{-1}. Compared with the LOD obtained by others' reports [34,35], the LOD of this interdigital electrode has surpassed

Please cite this article as: L. Wu et al., A new aptamer/black phosphorous interdigital electrode for malachite green detection, Analytica Chimica Acta, https://doi.org/10.1016/j.aca.2019.11.026

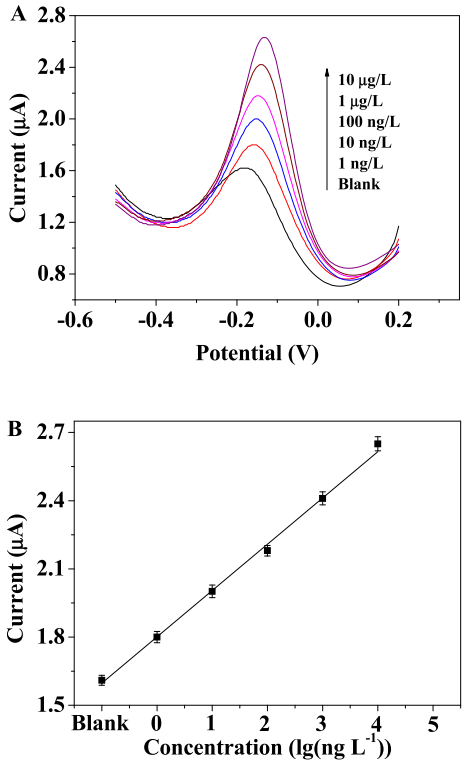

Fig. 3. (A) Differential pulse voltammograms (DPV) of the BP-AuNP-Ap interdigital electrode at different concentrations of MG from 1 ng L^{-1} to 10 μg L^{-1}, respectively. Pulse amplitude, 50 mV. (B) The increase of the peak current for MG at different concentrations from 1 ng L^{-1} to 10 μg L^{-1}, respectively. The standard deviations are all less than 5%.

that of the others (Table 1). It indicates that the functionalized BP plays a key role in improving the performances of the interdigital electrode.

The possible mechanism of MG identification by aptamer is shown in Scheme 1. There is a binding pocket in the MG aptamer which has the ability to recognize the MG molecules (Figure S4). Without the MG molecule, the single-strand aptamer immobilizes on the BP-AuNP nanocomposite through Au-S bond and behaves as a randomly coiled polymer. The MB molecule as signal sector also randomly exists on the surface of the BP-AuNP nanocomposite. In the presence of MG, the structure of aptamer changes and there is a binding pocket adapt to recognize MG. This binding pocket consists of a base quadruple (C7, G24, G29, A31), a Watson-Crick base pair (G8, C28) with two base triples (C10, G23, A27 and U11, A22, A26), and a U turn motif as the supporting framework. The structure of the aptamer with MG has shown in Figure S4. The aptamer with MG is more rigid than only the aptamer, which makes the MB signal molecule close to the surface of the BP-AuNP nanocomposite. This result is consistent with Thorsten Dieckmann's group report [36]. Thus, without MG, there is no significant response signal of this interdigital electrode. After the aptamer combines MG, a hairpin structure is formed [37]. The hairpin structure of the aptamer makes MB close to the electrode, and there is an obvious response signal. The high-conductivity BP with high loading capacity for MG significantly increases the LOD of the interdigital electrode.

Furthermore, the sensitivity of the BP-AuNP-Ap interdigital electrode, the AuNP-Ap interdigital electrode, the BP-Ap interdigital electrode, and the Ap interdigital electrode are 95.1, 71.75, 68.03 and 42.5 μA cm^{-2}, respectively. The peak currents of the AuNP-Ap interdigital electrode and the BP-Ap interdigital electrode exhibit a linear relationship from 100 ng L^{-1} to 10 mg L^{-1} and 1 μg L^{-1} to 10 mg L^{-1}, respectively (Figure S5). The linear regression equation of the AuNP-Ap interdigital electrode is $I = 0.0634C + 1.472$ ($R^2 = 0.999$), and that of the BP-Ap interdigital electrode is $I = 0.0611C + 1.406$ ($R^2 = 0.999$). The selectivity of the interdigital electrode is the ratio of the signal output with the analyte alone to that with the interfering substance alone. It is assessed by the co-existed interferents, i.e. chloramphenicol (CP), nitrofuran (NF) methyltestosterone (MTS) and eugenol (EG). As shown in Fig. 4A, the BP-AuNP-Ap interdigital electrode screen 4 types of the interferents at 10 ng L^{-1}. The response signal of MG is the strongest signal among these chemicals due to the excellent selectivity of the aptamer. The reproducibility is generally determined by the analyte concentration [38]. Fig. 4B is the response signals of the BP-AuNP-Ap interdigital electrode at 10 ng L^{-1} for 8 times, and the sampling interval is 30 min. The relative standard deviations of 8 times testing results are approximate 5%. This indicates that the functionalized BP is very stable in aqueous solution under output current, and it is not a single-use interdigital electrode.

3.4. Monitoring the aquaculture water samples by the BP-AuNP-Ap interdigital electrode

In this work, the BP-AuNP-Ap interdigital electrode is used for evaluating the aquaculture water samples from 7 provinces in China. The results show that only three aquaculture water samples have MG and the response signals increase 33%, 24%, and 16%, respectively. As shown in Fig. 4C and Table 2, the differences of the values are 23.5%, −26.1%, and −8.3%, respectively. It indicates that the results from the interdigital electrode are consistent with the LC-MS results. The developed interdigital electrode biosensor is an efficient tool for the selective determination of MG from coexisting aquaculture drugs even not very precise.

4. Conclusion

In this study, a simple method is developed to obtain the CYS-BP which can exist stably in aqueous solution for half a month. It overcomes the current disadvantage of BP. The stable BP is a promising biosensing platform to construct a novel BP-AuNP-Ap interdigital electrode for MG detection. The interdigital electrode biosensor shows a concentration-dependent response for MG with a low LOD and high selectivity. It is a useful pre-alarm tool for rapid and selective detection of MG in aquaculture water from coexisted drugs.

Table 1
Comparison of analytical performances of the BP-AuNP-Ap interdigital electrode with other methods for detection of MG. (PPy is the polypyrrole).

Modified biosensor	Linear range (ng/L)	Detection limit (ng/L)	Reference
BP-AuNP-Ap/Au interdigital electrode	$1.0-1.0 \times 10^4$	0.3	Present work
GP-AuNP-Ap-Chitosan/GC	$1.0 \times 10^2-1.0 \times 10^7$	16.3	[34]
PPy-Enzyme/CP	$2.5 \times 10^5-1.0 \times 10^7$	2.5×10^5	[35]

Please cite this article as: L. Wu et al., A new aptamer/black phosphorous interdigital electrode for malachite green detection, Analytica Chimica Acta, https://doi.org/10.1016/j.aca.2019.11.026

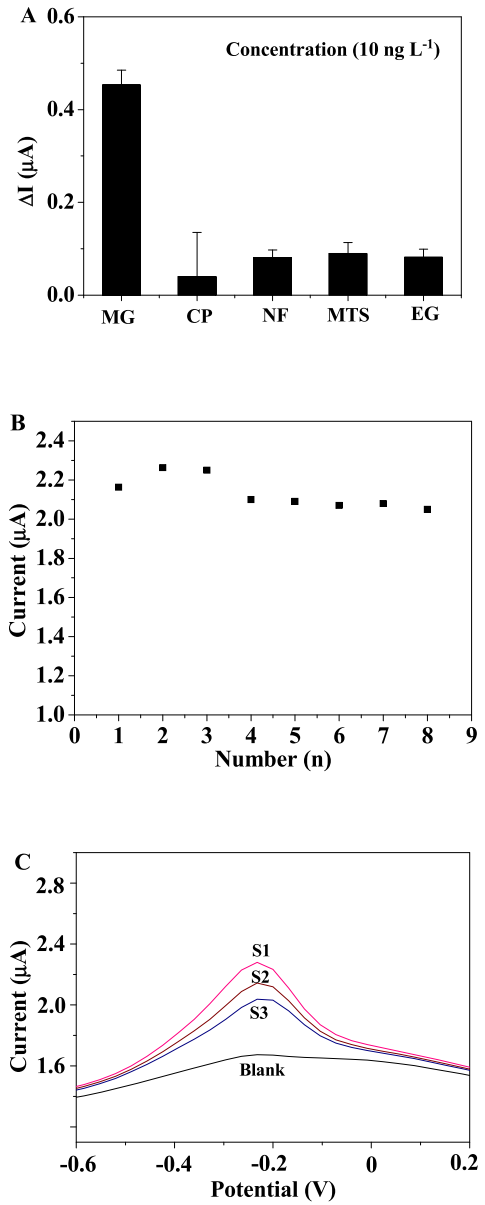

Fig. 4. (A) screening of MG, chloramphenicol (CP), nitrofuran (NF) methyltestosterone (MTS) and eugenol (EG) by the BP-AuNP-Ap interdigital electrode, (B) The reproducibility of the BP-AuNP-Ap interdigital electrode, and (C) Three real samples MG determination using the BP-AuNP-Ap interdigital electrode.

Table 2
Comparison of the determination of MG using the BP-AuNP-Ap interdigital electrode and LC-MS.

Sample	Concentration (ng L^{-1}) (Electrochemical method)	Concentration (ng L^{-1}) (LC-MS method)	Difference (%)[a]
1	10.5	8.5	23.5
2	8.5	11.5	−26.1
3	5.5	6.0	−8.3

[a] Difference=(Interdigital electrode $_{(value)}$-LC-MS$_{(value)}$)/LC-MS$_{(value)}$ × 100%.

Declaration of competing interest

The authors declare that they have no known competing financial interests or personal relationships that could have appeared to influence the work reported in this paper.

CRediT authorship contribution statement

Lidong Wu: Funding acquisition, Supervision, Writing - original draft, Writing - review & editing, Project administration. **Zhiyuan Xu:** Methodology, Writing - original draft. **Qingyi Meng:** Data curation. **Yushi Xiao:** Formal analysis. **Qiang Cao:** Data curation. **Brijesh Rathi:** Writing - review & editing. **Huan Liu:** Validation. **Gang Han:** Validation. **Jing Zhang:** Writing - review & editing. **Jiang Yan:** Writing - review & editing.

Acknowledgment

This work was supported by Central Public-interest Scientific Institution Basal Research Fund, CAFS (NO. 2019ZD08), the National Natural Science Foundation of China (No. 21307161 and 61874002) and Beijing Municipal Natural Science Foundation (No.4182021).

Appendix A. Supplementary data

Supplementary data to this article can be found online at https://doi.org/10.1016/j.aca.2019.11.026.

References

[1] X. Zhou, J. Zhang, Z. Pan, D. Li, Review of methods for the detection and determination of malachite green and leuco-malachite green in aquaculture, Crit. Rev. Anal. Chem. 49 (2019) 1–20.
[2] Z. Li, B. Tang, H. Zhang, Investigation on the interaction between an antimicrobial in aquaculture, malachite green and hemocyanin from mud crab Scylla paramamosain, Spectrochim. Acta A Mol. Biomol. Spectrosc. 135 (2015) 669–675.
[3] Y.H. Kim, C. Lee, H. Go, K. Konishi, K. Lee, P.C. Lau, M.H. Yu, Decolorization of malachite green by cytochrome c in the mitochondria of the fungus Cunninghamella elegans, Arch. Biochem. Biophys. 494 (2010) 159–165.
[4] S. Qiu, F. Zhao, O. Zenasni, J. Li, W.C. Shih, Nanoporous gold disks functionalized with stabilized G-quadruplex moieties for sensing small molecules, ACS Appl. Mater. Interfaces 8 (2016) 29968–29976.
[5] H. Li, J. Wang, X. Wang, H. Lin, F. Li, Perylene-based photoactive material as a double-stranded DNA intercalating probe for ultrasensitive photoelectrochemical biosensing, ACS Appl. Mater. Interfaces 11 (2019) 16958–16964.
[6] M. Eguilaz, R. Villalonga, G. Rivas, Electrochemical biointerfaces based on carbon nanotubes-mesoporous silica hybrid material: bioelectrocatalysis of hemoglobin and biosensing applications, Biosens. Bioelectron. 111 (2018) 144–151.
[7] J.S. Qiao, X.H. Kong, Z.X. Hu, F. Yang, W. Ji, High-mobility transport anisotropy and linear dichroism in few-layer black phosphorus, Nat. Commun. 5 (2014) 4475–4482.
[8] J.W. Jiang, H.S. Park, Negative Poisson's ratio in single-layer black phosphorus, Nat. Commun. 5 (2014) 4727–4734.
[9] B. Tian, B. Tian, B. Smith, M.C. Scott, R. Hua, Q. Lei, Y. Tian, Supported black phosphorus nanosheets as hydrogen-evolving photocatalyst achieving 5.4% energy conversion efficiency at 353 K, Nat. Commun. 9 (2018) 1397–1408.
[10] L. Bai, X. Wang, S. Tang, Y. Kang, J. Wang, Y. Yu, Z.K. Zhou, C. Ma, X. Zhang, J. Jiang, P.K. Chu, X.F. Yu, Black phosphorus/platinum heterostructure: a highly efficient photocatalyst for solar-driven chemical reactions, Adv. Mater. 30 (2018) 1803641–1803648.
[11] S.J.R. Tan, I. Abdelwahab, L. Chu, S.M. Poh, Y. Liu, J. Lu, W. Chen, K.P. Loh, Quasi-monolayer black phosphorus with high mobility and air stability, Adv. Mater. 30 (2018) 1704619–1704627.
[12] A.N. Abbas, B.L. Liu, L. Chen, Y.Q. Ma, S. Cong, N. Aroonyadet, M. Kopf, T. Nilges, C.W. Zhou, Black phosphorus gas sensors, ACS Nano 9 (2015) 5618–5624.
[13] C.M. Chen, J. Xu, Y. Yao, SIW resonator humidity sensor based on layered black phosphorus, Electron. Lett. 53 (2017).
[14] F. Ahmed, Y.D. Kim, Z. Yang, P. He, E. Hwang, H. Yang, J. Hone, W.J. Yoo, Impact ionization by hot carriers in a black phosphorus field effect transistor, Nat. Commun. 9 (2018) 3414.
[15] X. Chen, C. Chen, A. Levi, L. Houben, B. Deng, S. Yuan, C. Ma, K. Watanabe, T. Taniguchi, D. Naveh, X. Du, F. Xia, Large-velocity saturation in thin-film black phosphorus transistors, ACS Nano 12 (2018) 5003–5010.
[16] Y.T. Chen, R. Ren, H.H. Pu, J.B. Chang, S. Mao, J.H. Chen, Field-effect transistor biosensors with two-dimensional black phosphorus nanosheets, Biosens. Bioelectron. 89 (2017) 505–510.
[17] Q. Zhao, W. Ma, B. Pan, Q. Zhang, X. Zhang, S. Zhang, B. Xing, Wrinkle-induced high sorption makes few-layered black phosphorus a superior adsorbent for ionic organic compounds, Environ. Sci.: Nano 5 (2018) 1454–1465.
[18] J. Plutnar, Z. Sofer, M. Pumera, Products of degradation of black phosphorus in

protic solvents, ACS Nano 12 (2018) 8390–8396.
[19] T. Zhang, Y. Wan, H. Xie, Y. Mu, P. Du, D. Wang, X. Wu, H. Ji, L. Wan, Degradation chemistry and stabilization of exfoliated few-layer black phosphorus in water, J. Am. Chem. Soc. 140 (2018) 7561–7567.
[20] C.J. An, Y.H. Kang, C. Lee, S.Y. Cho, Preparation of highly stable black phosphorus by gold decoration for high-performance thermoelectric generators, Adv. Funct. Mater. 28 (2018) 1800532–1800539.
[21] D.H. Kwak, H.S. Ra, J. Yang, M.H. Jeong, A.Y. Lee, W. Lee, J.Y. Hwang, J.H. Lee, J.S. Lee, Recovery mechanism of degraded black phosphorus field-effect transistors by 1,2-ethanedithiol chemistry and extended device stability, Small 14 (2018) 1703194–1703201.
[22] J. Na, Y.T. Lee, J.A. Lim, D.K. Hwang, G.T. Kim, W.K. Choi, Y.W. Song, Few-layer black phosphorus field-effect transistors with reduced current fluctuation, ACS Nano 8 (2014) 11753–11762.
[23] Y. Zhao, Y.H. Zhang, Z. Zhuge, Y.H. Tang, J.W. Tao, Y. Chen, Synthesis of a poly-l-lysine/black phosphorus hybrid for biosensors, Anal. Chem. 90 (2018) 3149–3155.
[24] Y. Cao, X. Tian, J. Gu, B. Liu, B. Zhang, S. Song, F. Fan, Y. Chen, Covalent functionalization of black phosphorus with conjugated polymer for information storage, Angew. Chem. 57 (2018) 4543–4548.
[25] C.R. Ryder, J.D. Wood, S.A. Wells, Y. Yang, D. Jariwala, T.J. Marks, G.C. Schatz, M.C. Hersam, Covalent functionalization and passivation of exfoliated black phosphorus via aryl diazonium chemistry, Nat. Chem. 8 (2016) 597–602.
[26] B. Gulbakan, K. Barylyuk, P. Schneider, M. Pillong, G. Schneider, R. Zenobi, Native electrospray ionization mass spectrometry reveals multiple facets of aptamer-ligand interactions: from mechanism to binding constants, J. Am. Chem. Soc. 140 (2018) 7486–7497.
[27] H. Mei, J.Y. Liao, R.M. Jimenez, Y. Wang, S. Bala, C. McCloskey, C. Switzer, J.C. Chaput, Synthesis and evolution of a threose nucleic acid aptamer bearing 7-deaza-7-substituted guanosine residues, J. Am. Chem. Soc. 140 (2018) 5706–5713.
[28] L. Wang, Y. Wang, J.I. Wong, T. Palacios, J. Kong, H.Y. Yang, Functionalized MoS2 nanosheet-based field-effect biosensor for label-free sensitive detection of cancer marker proteins in solution, Small 10 (2014) 1101–1105.
[29] S.L. Stead, H. Ashwin, B. Johnston, J.A. Tarbin, M. Sharman, J. Kay, B.J. Keely, An RNA-aptamer-based assay for the detection and analysis of malachite green and leucomalachite green residues in fish tissue, Anal. Chem. 82 (2010) 2652–2660.
[30] X. Zhang, M. Wang, L. Lin, G. Xiao, Z. Tang, X. Zhu, Synthesis of novel laccase-biotitania biocatalysts for malachite green decolorization, J. Biosci. Bioeng. 126 (2018) 69–77.
[31] J.X. Dong, C. Xu, H. Wang, Z.L. Xiao, S.J. Gee, Z.F. Li, F. Wang, W.J. Wu, Y.D. Shen, J.Y. Yang, Y.M. Sun, B.D. Hammock, Enhanced sensitive immunoassay: noncompetitive phage anti-immune complex assay for the determination of malachite green and leucomalachite green, J. Agric. Food Chem. 62 (2014) 8752–8758.
[32] Q. Zhou, Q. Chen, Y. Tong, J. Wang, Light-Induced ambient degradation of few-layer black phosphorus: mechanism and protection, Angew. Chem. 55 (2016) 11437–11441.
[33] W.S. Chen, J. Ouyang, H. Liu, M. Chen, K. Zeng, J.P. Sheng, Z.J. Liu, Y.J. Han, L.Q. Wang, J. Li, L. Deng, Y.N. Liu, S.J. Guo, Black phosphorus nanosheet-based drug delivery system for synergistic photodynamic/photothermal/chemotherapy of cancer, Adv. Mater. 29 (2017) 1603864–1603871.
[34] J.R. Babendure, S.R. Adams, R.Y. Tsien, Aptamers switch on fluorescence of triphenylmethane dyes, J. Am. Chem. Soc. 125 (2003) 14716–14717.
[35] A. Swarbrick, E.J. Murby, P. Hume, Post-column electrochemical oxidation of leuco malachite green for the analysis of rainbow trout flesh using HPLC with absorbance detection, J. Liq. Chromatogr. Relat. Technol. 20 (1997) 2269–2280.
[36] J.B. Da Costa, A.I. Andreiev, T. Dieckmann, Thermodynamics and kinetics of adaptive binding in the malachite green RNA aptamer, Biochemistry-Us 52 (2013) 6575–6583.
[37] B.Q. Wang, S.J. Dong, Organic-phase enzyme electrode for phenolic determination based on a functionalized sol-gel composite, J. Electroanal. Chem. 487 (2000) 45–50.
[38] D.R. Thevenot, K. Toth, R.A. Durst, G.S. Wilson, Electrochemical biosensors: recommended definitions and classification, Biosens. Bioelectron. 16 (2001) 121–131.

Please cite this article as: L. Wu et al., A new aptamer/black phosphorous interdigital electrode for malachite green detection, Analytica Chimica Acta, https://doi.org/10.1016/j.aca.2019.11.026